

# Characteristics of Microscopic Proton Current Flow Distributions in Fresh and Aged Nafion Membranes

Osung Kwon,<sup>†</sup> Yihong Kang,<sup>†</sup> Shijie Wu,<sup>‡</sup> and Da-Ming Zhu<sup>\*,†</sup>

Department of Physics, University of Missouri—Kansas City, Kansas City, Missouri 64110, and Agilent Technologies, Inc., 4330 West Chandler Boulevard, Chandler, Arizona 85282

Received: November 24, 2009; Revised Manuscript Received: January 29, 2010

Proton conductance in fresh and aged Nafion ionomer membranes has been studied using current sensing atomic force microscopy which measures the proton current flow from a nanometer-sized tip in contact with the membrane surface to an electrode attached to the other side of the membrane. By scanning the tip across the membrane, the measured conductance maps out the local proton conductance variations, revealing the distributions of ionic domains on the membrane surface. For fresh Nafion membranes, the local proton conductance always displays a single-peaked distribution, while, for membranes after being aged for about three years in an ambient environment, the local proton conductance shows a distribution with two peaks, one at high current corresponding to the variation of contact and the conductive path of proton current and the other at near zero current which corresponds to the appearance of large nonconductive domains on the membranes. A detailed analysis reveals that the aging causes significant changes in the ionic domains or channels exposed on the membranes' surfaces.

## 1. Introduction

Although significant progress has been made over the past decade in the development of highly efficient and reliable fuel cell technologies, a full scale commercialization of fuel cells in various types of applications remains a challenging task.<sup>1–5</sup> One of the technical barriers for using fuel cells to replace currently employed energy devices is their limited durability and stability under a wide range of operational conditions.<sup>5–7</sup> Among many factors that influence the durability of a fuel cell, the degradation of the key components, such as the electrolyte and electrode assembly, plays an important role in determining the performance of a fuel cell.<sup>6–8</sup> For polymer electrolyte membrane (PEM) fuel cells, the aging of the polymer electrolyte membrane is probably intrinsic to the material; such a property would lead to degradation of the fuel cell and cause deterioration of the cell's performance. In order to mitigate the degradation of polymer electrolyte membrane and to obtain guidance for developing new membrane materials with improved reliability and durability properties, it is important to elucidate the aging process at a microscopic level and to understand the aging mechanisms of polymer electrolyte membranes.

Currently, the most commonly used membranes in polymer electrolyte fuel cell developments is Nafion, which represents a family of commercially available membranes consisting of comb-shaped ionomers with a perfluorinated polymeric backbone and short side chains that terminate in hydrophilic sulfonic acid head groups ( $-\text{SO}_3\text{H}$ ).<sup>9–26</sup> These groups and water molecules organize into hydrophilic and nanometer sized domains which leads to unique permeability characteristics of the membranes. While a number of alternative polymer membranes have been developed in recent years, Nafion membranes are still considered the state-of-the-art membrane materials for PEM

fuel cells and the benchmark materials against which most results are compared.<sup>9–26</sup> The structure of Nafion membranes is complex and intrinsically heterogeneous.<sup>9–26</sup> Despite a long history of research and a number of successful applications of the membranes, their morphology remains the focus of debate in the current literature.<sup>9–28</sup> Nevertheless, a number of phenomenological models have been proposed for describing the structures of Nafion membranes.<sup>11–26</sup> A semiempirical view based on these models considers a Nafion membrane a phase separated morphology consisting of discrete hydrophobic and hydrophilic domains; the polymer fluorocarbon backbones and side chains form hydrophobic domains, while the ionic groups and their counterions make up the hydrophilic domains which attract water molecules, as illustrated in Figure 1 (the colored regions are hydrophilic domains).<sup>13–15,21–25</sup> As the water content in the membrane increases, the hydrophilic domains increase their sizes, and eventually percolate through the membrane, forming a random ionic conducting channel network and providing a continuous pathway for ionic conduction.<sup>13–15,21–25</sup> The results from the studies using small-angle X-ray scattering and neutron scattering, transmission electron microscopy, and, recently, scanning probe microscopy indeed revealed a nanometer-sized phase-separated morphology structure in Nafion.<sup>14,15,27–29</sup> A recent study finds that the existing experimental data can be consistently explained in terms of a model that describes the structure of Nafion membrane comprising arrays of ionic nanometer-sized channels oriented in parallel and embedded in a locally aligned polymer matrix.<sup>12</sup> The array of ionic channels swells perpendicular to the bundle direction when the membrane is hydrated, which allows protons to diffuse easily in this tubular nanostructure.<sup>12</sup>

An important question arises as to whether and how these ionic domain and channel structures change in the membrane's aging process. Previous studies found the properties of Nafion membranes, including ionic transport properties, deteriorate significantly over their aging processes.<sup>30–35</sup> Since the microscopic structures of Nafion membranes are heterogeneous, it is

\* Corresponding author. E-mail: zhud@umkc.edu. Phone: (816)235-5326. Fax: (816)235-5221.

<sup>†</sup> University of Missouri—Kansas City.

<sup>‡</sup> Agilent Technologies, Inc.

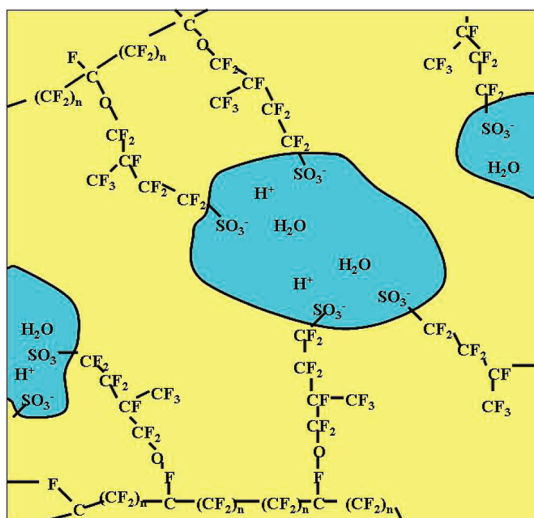


**Figure 1.** Illustration of hydrophilic and hydrophobic domains in a Nafion membrane. Hydrophilic sulfonic acid head groups ( $-SO_3^-$ ) combined with water molecules form hydrophilic domains (blue colored), and these domains become connected at a higher hydration state, forming an ionic channel network.

conceivable that an aging process would not proceed uniformly in the membrane and the degradation mechanisms might be correlated with the heterogeneous nature of the membrane's structure. In this paper, we present results of a study which investigated proton transport properties in aged and fresh Nafion membranes using current sensing atomic force microscopy (CSAFM). The results reveal that proton current flow distribution in aged membranes is characteristically different from that in fresh membranes. The local proton conductance of the membrane becomes significantly nonuniform with the sizes of nonconductive domains being significantly increased, resulting in a characteristic double peaked local proton conductance distribution measured with CSAFM. A detailed analysis of the distribution reveals that the proton conducting channels in the aged membranes are crumpled together, forming large channels, leaving the surrounding area nonconductive.

## 2. Experimental Section

Local probes, such as scanning probe microscopes, are powerful tools for studying surface structures as well as materials with heterogeneous structures.<sup>36–43</sup> Since ion transport property is not uniform across regions consisting of hydrophilic and hydrophobic domains in a Nafion membrane, it is desirable to directly probe the ionic activity and ionic conductivity at a scale over which the ionic transport properties in these domains can be distinguished. It is also preferable that the study is conducted under conditions that mimic those for fuel cell operation. Indeed, atomic force microscopy (AFM) has been used in the studies of ion exchange membranes under different environments, and the cluster structures of the membranes and their evolvement with external conditions have been demonstrated.<sup>36–43</sup> In recent years, current sensing atomic force microscopy (CSAFM), a novel AFM technique that can be used to probe simultaneously the surface morphology and the local conductance variation of a sample, has been employed in studies of Nafion membranes.<sup>36–40</sup> The essential component in a CSAFM, aside from those in conventional AFMs, is a sensitive electric current measuring loop which connects a conducting probe tip and the sample.<sup>37–39</sup> The probe tip is usually a conventional AFM tip coated with a uniform metal layer which

acts as the current sensor. For imaging the current flow in proton exchange membranes, the metal layer also acts as the catalyst; thus, usually a layer of platinum is used. The CSAFM probe tip serves as an electrode and is in contact with the bare surface of the membrane; the other surface of the membrane is attached with a catalyst (platinum) filled carbon cloth which serves as another electrode and is connected to the probe tip through the current sensing loop. The tip/Pt/Nafion/Pt/carbon assembly forms a miniature fuel cell assembly.

As a CSAFM probe tip scans across the surface of a membrane in contact mode, the tip traces out the surface morphology and, at the same time, senses proton current flow between the contact of the tip and the plane electrode on the other side of the membrane, generating simultaneously a surface morphology and current sensing images. The sensed current depends sensitively on the contact between the probe tip and ionic channels in the membrane. In principle, it is possible to resolve individual proton conducting channels using CSAFM if the probe tip used is sharp enough. However, due to the softness of Nafion membrane and water condensation under a fuel cell's operation conditions, the contact area between the probe tip and the membrane usually is much larger than the size of a single ionic cluster or channel on the membrane, making resolving an individual ionic channel difficult.<sup>39</sup> However, the ionic conductance distribution derived from the current sensing images reveals indirectly the averaged size of ion conducting clusters on a membrane surface and the ionic current flow from a single cluster contact with the tip to the plane.<sup>39</sup> If an ionic channel branches out or merges with other channels over a distance much smaller than the thickness of the membrane, the ion flow from a single channel in contact with the tip would spread over a large portion of the ionic channel network across the membrane before reaching the electrode on the other surface of the membrane. Assuming the ionic channel network in a Nafion membrane is completely random, the variation due to conductance across the membrane is averaged out; the contact between the tip and the ionic clusters on the membrane surface would determine the magnitude of ionic current measured. Using a contact mode, the force applied to the membrane during imaging is kept constant by adjusting the vertical position of the probe tip following the surface profile; such a constant force mode would maintain a constant contact area between the tip and the membrane surface. Thus, the current sensing image would be dominated by the variation of the contact between the probe tip and ionic clusters or channels on the membrane surface. If the sizes of ionic clusters or channels exposed on the membrane surface are uniform, the measured conductance at different pixels would follow a Poisson distribution which reflects the probability of discrete number of channels in contact with the tip.<sup>44</sup> However, due to the disorder in the microscopic structure of the membrane, the sizes and shapes of the clusters or channels are irregular, the distribution at each integer number of channels becomes broadened. For clusters or channels with sufficient disorder, the distribution may evolve to a continuous one which can be approximately described as a Gaussian, with the width of the distribution dictated by the original Poisson distribution.<sup>44</sup> Under these assumptions, the averaged proton current flow from a single cluster on the membrane surface in contact with the probe tip to the opposite electrode  $\sigma$ , and the averaged number of the contacting clusters with the tip  $\lambda$  can be related to the peak value,  $C_{\text{peak}}$ , and the full width at half-maximum (fwhm),  $\Delta C$ , of the conductance distribution by<sup>39</sup>

$$C_{\text{peak}} = \lambda \cdot \sigma \quad (1)$$

$$\Delta C = 2\sqrt{2 \ln 2} \cdot \sqrt{\lambda} \cdot \sigma \quad (2)$$

In the case where the contact area is comparable or smaller than the size of ionic clusters and the space between them, the tip is either in contact with one cluster or not in contact with any cluster at all, the distribution should display two peaks, with one at near zero current.<sup>39</sup>

In this work, several pieces of fresh and aged Nafion membranes were studied using two different CSAFM instruments.<sup>45</sup> The Nafion membrane samples were obtained directly from DuPont and from a fuel cell supply manufacturer.<sup>46,47</sup> The membranes were hot-pressed onto a carbon cloth covered with a thin layer of Nafion solution mixed with Pt powder. The other surfaces of the membranes were kept clean. The fresh membrane samples were imaged within two months after they were received from the manufacturer, while the aged membrane samples were kept in a clean and sealed sample box which was placed in an ambient laboratory environment for three years. To perform current sensing imaging, the membrane electrode assembly was placed in a CSAFM (PicoScan, Agilent Technology)<sup>45</sup> sample stage which was housed inside an environmental chamber in which the relative humidity was precisely monitored and controlled through a vapor pressure handling system, and then the carbon electrode substrate was connected with the current sensing loop in the CSAFM. When the probe tip (coated with Pt) is in contact with the clean surface of the membrane, a tip/Pt/Nafion/Pt/carbon assembly is formed.<sup>37–39</sup> A 1.5 bias voltage was applied to the probe tip against the carbon electrode substrate to initiate electrolysis of water to generate hydrogen. All of the imaging and the measurements were carried out at room temperature, and a detailed description about the experimental conditions can be found in previous publications.<sup>37–39</sup> A more updated model of CSAFM (Agilent 5500)<sup>45</sup> was used at the end of the study, and the results show that major features obtained using the two CSAFMs are similar.

### 3. Results and Discussion

The topographic images obtained on the aged membranes do not show a significant difference from those on fresh membranes which have been reported in our previous publications,<sup>37–39</sup> and thus will not be discussed in detail here. In contrast, significant differences in proton current sensing images obtained simultaneously with the topographic images are shown on the fresh and aged membranes. Figure 2a and b displays typical current sensing images obtained on a fresh and an aged Nafion NR 212 membrane sample under the same conditions (room temperature and a relative humidity of 55%). The characteristic difference in the spatial variation in local proton current flow can be more clearly seen in the current profiles obtained along the lines in the images; these profiles are depicted in Figure 2c and 2d. Comparing to the detected proton current profile of the fresh membrane, the profile in the aged membrane shows much larger nonconductive areas with the sizes ranging from tens of nanometers to about a few micrometers, as can be seen in the figure, in contrast to the situation of a fresh membrane in which the sizes of ionic clusters or channels are typically a few nanometers in diameter.<sup>11–24</sup> As described above, the significant size differences of nonconductive regions in the fresh and aged membranes should result in a completely different behavior in the local proton flow current distribution which is the collection of proton currents measured at each pixel. For fresh Nafion

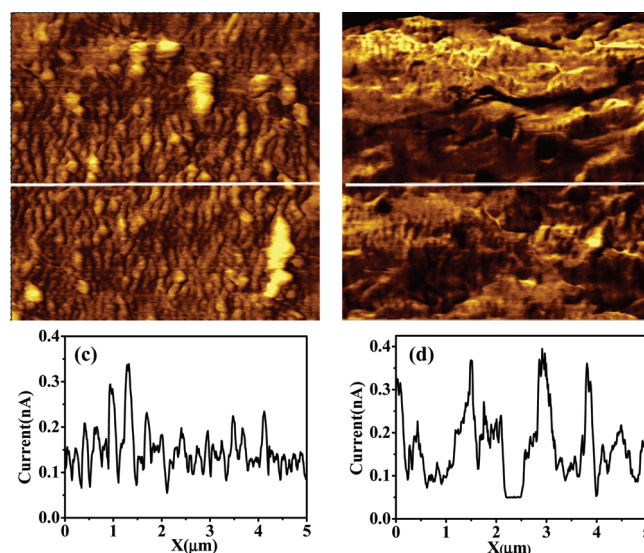


**Figure 2.** Current sensing atomic force microscopy (CSAFM) images on a fresh Nafion NR212 membrane (a) and on an aged Nafion NR212 membrane (b). The imaging conditions were identical (room temperature under a 55% relative humidity). (c and d) Proton current profiles on the sample along the line scan indicated in images a and b, respectively.

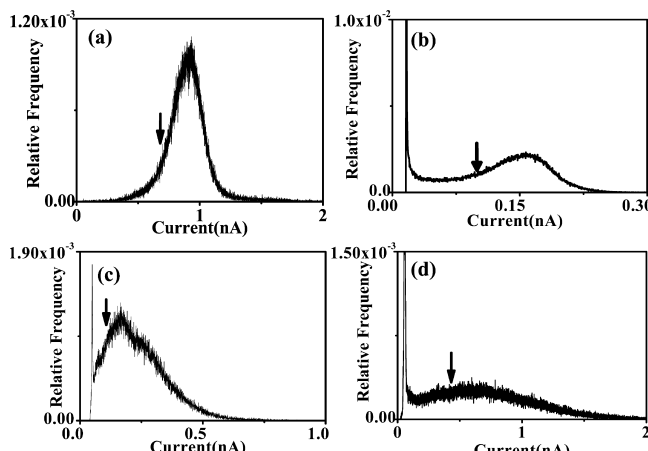


**Figure 3.** (a) Proton current flow distribution on a fresh Nafion NR 212 membrane measured using a CSAFM under a relative humidity of 75%. (b–d) Proton current flow distributions on aged Nafion NR 212 membranes at relative humidities of 50, 55, and 75%, respectively. The distributions in parts c and d were measured using a PicoScan, while the distribution in part b was obtained using an Agilent 5500 instrument.

membranes, the proton current flow distributions are always single peaked, with the peak value and the width varying with the relative humidity of the sample chamber.<sup>37,38</sup> Figure 3a displays such a distribution obtained on a fresh Nafion NR212 membrane imaged at room temperature under a relative humidity of 75%. At a lower relative humidity, the distribution shape remains the same but the peak shifts toward a lower current.<sup>38,39</sup> Shown in parts b–d are the proton current flow distributions on aged Nafion NR 212 membranes under different relative humidities. Comparing to that for a fresh membrane, a distinct feature in the current flow distributions obtained on the aged membrane is that they show two peaks, one at near zero current and the other at higher current with a broad distribution; the peak at the higher current has an asymmetric shape with a shoulder extending toward the low current values. Obviously, the distribution peak at near zero current comes from the nonconductive regions. To demonstrate these characteristics

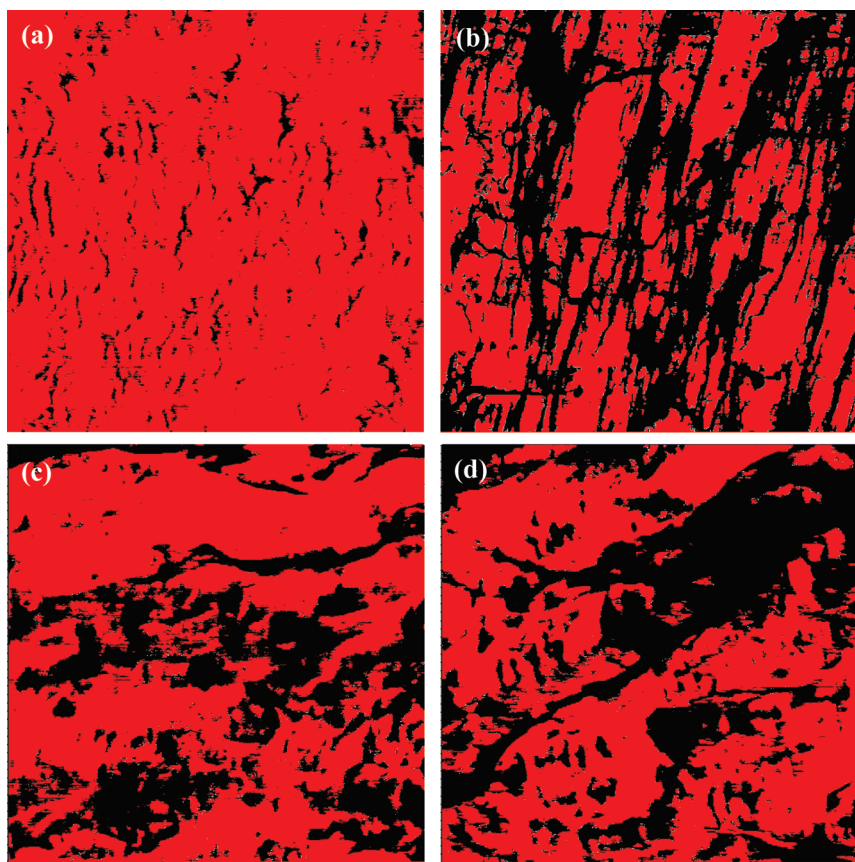


**Figure 4.** Low current (black region) and high current (red region) contour maps for the four images, of which the current flow distributions are displayed in Figure 3, with the cut-off current set at the values indicated in the distribution plots in Figure 3.

more clearly, we plot in Figure 4 the regions in the current images over which the proton current detected are below a cutoff value, which is defined as the current at the lower half-maximum height of the distribution, indicated in the distribution in Figures 3, in black, while the rest of the region in red. These images present contour maps of good and poor proton conductive regions and show that the distribution of these regions is characteristically different on the fresh and aged Nafion membranes. Figure 4a shows such a contour map on a fresh Nafion NR212 membrane, while Figure 4b–d shows the nonconducting contour maps for the aged Nafion NR212 membranes at different relative humidity. The nonconductive regions in the aged membranes appear to aggregate together, forming nonconductive strips.

Similar to that found in fresh membranes, the proton current flow distribution in the aged Nafion membrane also depends on the relative humidity, and thus the hydration state of the membrane. As the hydration decreases, the high current peaks shift toward lower current and eventually merge with the near zero current peak, as shown in Figure 3. In Figure 5, we plot the peak values of the proton current flow distribution of the fresh and the aged Nafion membranes at different relative humidities. The overall behaviors of the nonzero current peaks in the current flow distribution as a function of relative humidity for the fresh and the aged membranes are consistent with that observed in studies using macroscopic methods,<sup>48</sup> and are similar to each other except for the fact that the peak values of the fresh membranes appear to increase faster with the relative humidity.<sup>38,39,48</sup> Integrating over the proton current flow distribution and multiplying a geometric scaling factor yields proton conductance between the tip and plane electrode for the aged membrane ( $\sigma_a$ ) and for the fresh membrane ( $\sigma_f$ ), respectively.

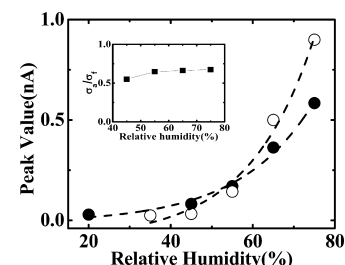


**Figure 5.** Peak values of the proton current flow distribution for a fresh Nafion NR 212 membrane (○) and an aged Nafion NR 212 membrane (●), as a function of relative humidity. The inset displays the ratio of the conductance integrated areas under the current distributions for the aged and fresh membranes. The ratio shows that the proton conductivity in aged membrane decreases by about 30%. The lines are guides to the eye.

The ratios of the integrated conductance peaks ( $\sigma_a/\sigma_f$ ) of the aged and the fresh membranes at different relative humidities are plotted in the inset of Figure 5, which demonstrates that aging in Nafion NR212 membranes at room temperature in ambient environment over a period of about three years causes degradation in proton conductivity by about 30%.

As described above, CSAFM measures proton current flow from a probe tip through a random ionic channel network in a membrane to a plane electrode plated on the opposite surface of the membrane. The conductance variation can be caused by both the contact between the probe tip and the proton channels exposed on the bare surface of the membrane and the conductive path from the probe tip to the plane electrode on the other side of the membrane. A recent simulation study based on small-angle X-ray and neutron scattering data on Nafion membranes concluded that the ionic clusters in the membranes are in the

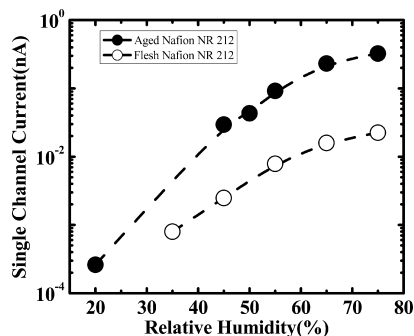


**Figure 6.** Comparison of the proton current flow from a single ionic channel in contact with the probe to the plane electrode on the other side of the membrane, derived from the proton current flow distribution using eqs 1 and 2, for fresh and aged membranes as a function of relative humidity.

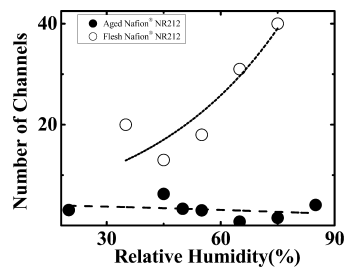


**Figure 7.** Comparison of the number of proton channels in contact with the probe tip, derived from the proton current flow distribution using eqs 1 and 2, for fresh and aged membranes as a function of relative humidity.

form of ion channels orientated mostly in parallel with each other with length on the order of a few hundred nanometers,<sup>12</sup> much smaller than the thickness of the Nafion NR 212 membrane which is about 50  $\mu\text{m}$ .<sup>46</sup> Assuming that the ends of ion channels are randomly connected, the proton conducting path branches out or emerges with other channels over the length of each individual channel. Thus, the current flow from a probe tip to the plane electrode of the other side of the membrane spreads over a large number of branches of the network, and the variation of the current path in the proton channel network as the probe tip is located at a particular position on the surface of the membrane is averaged out. Therefore, the conductance variation probed by the CSAFM reflects mainly the contact probability of the probe tip and the proton channels. Such a contact probability is related to surface ionic activity of the membrane.<sup>37</sup> Using the arguments presented in section 2, the current flow from a single channel in contact with the probe  $\sigma$  and the averaged number of the channels  $\lambda$  in contact with the probe tip can be determined from the peak position  $C$  and the full width at half-maximum  $\Delta C$  of the distribution, following eqs 1 and 2. In Figures 6 and 7, the averaged current flow from a single proton channel in contact with the CSAFM tip to the plane electrode on the other side of the membrane,  $\sigma$ , and the averaged number of the proton channels in contact with the tip,  $\lambda$ , derived using eqs 1 and 2, are plotted as a function of relative humidity for both the aged and the fresh membranes. The current flow from a single proton channel in the aged membrane appears to be larger than that in the fresh membrane, while the number of channels in contact with the tip for the aged membrane is significantly less than that for the fresh membrane. Assuming that the CSAFM tip we used has a radius of 20 nm and the water meniscuses around the tip apex can be described by the Kelvin equation, we calculated the contact area between the tip and the membrane using a contact mechanics model.<sup>39</sup> Using

the contact area and the averaged number of ionic clusters in contact with the tip derived from the current distribution, we obtained an averaged nearest neighbor distance between ion clusters of 5.3 nm for the fresh membranes.<sup>39</sup> Such a value is comparable to that obtained in recent simulation and small-angle X-ray scattering work.<sup>12,39,49</sup> It is very unlikely that any mechanism could cause an increase of the current flow through a single channel other than the possibility that the size of the proton channel is enlarged by aggregating several proton channels close together, forming a larger one. This mechanism explains the significant decrease in the number of channels in contact with the tip for the aged membranes. It is intriguing to note that while the number of channels in contact with the CSAFM tip increases with relative humidity for fresh membranes, probably due to increased water meniscus at the contact region, it remains about the same for the aged membranes. Overall, the results we have obtained strongly suggest that, as a Nafion membrane ages, some ionic clusters or proton channels disappear; those remaining ionic clusters and channels clump together, forming larger clusters or channels. The overall reduction in proton conductivity suggests that the degradation should be mainly caused by the changes of sulfonic acid group terminated side chains in the Teflon backbone structure.<sup>30</sup> However, the characteristic changes in the morphology of ionic active domains on the membrane surface due to aging remain to be explained and understood. It will be particularly interesting to investigate the variation in the chemical composition in the low and high conductive regions using various spectroscopic approaches and to identify the microscopic origin of the proton conductive degradation mechanism in the aging process of Nafion membranes.

### Summary

We have studied proton transport properties of fresh and aged Nafion membranes using current sensing atomic force microscopy to reveal changes of the ionic domains and the local ionic conductivity distribution in the membranes due to aging. The results show that the current mapping obtained using current sensing AFM on aged membranes are characteristically different from that obtained on fresh membranes. The local conductance in the aged membranes becomes drastically more nonhomogenous, with domains of sizes up to several hundred nanometers being completely nonconductive and these domains appear to aggregate together, forming strips. These nonconductive domains result in a sharp peak near the zero current in the conductance distribution derived from the current sensing images. The conductive domains in the aged membrane show a dependence on the hydration state of the membranes similar to that found in fresh membrane, but the overall conductivity is reduced by about 30%. Further analysis finds evidence which suggests that the proton conducting channels in the aged Nafion membranes become larger channels. Consequently, the averaged number of channels in contact with the probe tip is significantly reduced, suggesting that proton conducting channels aggregate together, forming larger channels in the aging process. These results demonstrate that ionic conductance mapping using current sensing atomic force microscopy can yield information on the microscopic changes in the ionic channels in the aging process, which may shed light on the fundamental mechanisms of the aging mechanisms for Nafion membranes.

**Acknowledgment.** We would like to thank Doug Ewart at DuPont for supplying us with Nafion membrane samples. This work is supported in part by Research Corporation, Kansas City Life Science Inc., and University of Missouri Research Board.

## References and Notes

- (1) For reviews, see: O’Hayre, R.; Colella, W.; Cha, S.-W.; Fritz, B.; Prinz, F. G. *Fuel Cell Fundamentals*, 2nd ed; John Wiley & Sons: New York, 2009.
- (2) Srinivasan, S. *Fuel Cells: from Fundamentals to Applications*; Springer Science and Business, LLC: New York, 2006.
- (3) Mehta, V.; Cooper, J. S. Review and analysis of PEM fuel cell and manufacturing. *J. Power Sources* **2003**, *114*, 21–53.
- (4) Gottesfeld, S.; Zawodzinski, T. A. Polymer Electrolyte Fuel Cells. In *Advances in Electrochemical Science and Engineering*; Alkire, R. C., Gerischer, H., Kolb, D. M., Tobias, C. W., Eds.; Wiley-VCH: Weinheim, Germany, 1997; Vol. 5, pp 195–301.
- (5) Beuscher, U.; Cleghorn, S. J. C.; Johnson, W. B. *Int. J. Energy Res.* **2005**, *29*, 1103–1112.
- (6) Wu, J.; Yuan, X. Z.; Martin, J. J.; Wang, H.; Zhang, J.; Shen, J.; Wu, S.; Merida, W. *J. Power Sources* **2008**, *184*, 104–119.
- (7) Perrot, C.; Meyer, G.; Gonon, L.; Gebel, G. *Fuel Cell* **2006**, *1*, 10–15.
- (8) Knights, S. D.; Colbow, K. M.; St-Pierre, J.; Wilkinson, D. P. *J. Power Sources* **2004**, *127*, 127–134.
- (9) Mauritz, K.; Moore, R. B. *Chem. Rev.* **2004**, *104*, 4535–4586.
- (10) Hickner, M. A.; Ghassemi, H.; Kim, Y. S.; Einsla, B. R.; McGrath, J. E. *Chem. Rev.* **2004**, *104*, 4587–4612.
- (11) van der Heijden, P. C.; Rubat, L.; Diat, O. *Macromolecules* **2004**, *37*, 5327–5336.
- (12) Schmidt-Rohr, K.; Chen, Q. *Nat. Mater.* **2008**, *7*, 75–83.
- (13) Hsu, W. Y.; Gierke, T. D. *J. Membr. Sci.* **1983**, *13*, 307–326.
- (14) Fujimura, M.; Hashimoto, T.; Kawai, H. *Macromolecules* **1981**, *14*, 1309–1315.
- (15) Fujimura, M.; Hashimoto, T.; Kawai, H. *Macromolecules* **1982**, *15*, 136–144.
- (16) Dreyfus, B.; Gebel, G.; Aldebert, P.; Pineri, M.; Escoubes, M.; Thomas, M. *J. Phys. (Paris)* **1990**, *51*, 1341–1354.
- (17) Fujimura, M.; Hashimoto, T.; Kawai, H. *Macromolecules* **1982**, *15*, 136–144.
- (18) Gebel, G.; Moore, R. B. *Macromolecules* **2000**, *33*, 4850–4855.
- (19) Gebel, G.; Lambard, J. *Macromolecules* **1997**, *30*, 7914–7920.
- (20) Rollet, A. L.; Gebel, G.; Simonin, J. P.; Turq, P. *J. Polym. Sci., Part B: Polym. Phys.* **2001**, *39*, 548.
- (21) Litt, M. H. *Polym. Prepr.* **1997**, *38*, 80–81.
- (22) Haubold, H. G.; Vad, T.; Jungbluth, H.; Hiller, P. *Electrochim. Acta* **2001**, *46*, 1559–1563.
- (23) Rubat, L.; Rollet, A. L.; Gebel, G.; Diat, O. *Macromolecules* **2002**, *35*, 4050–4055.
- (24) Gierke, T. D.; Munn, G. E.; Wilson, F. C. *J. Polym. Sci., Part B: Polym. Phys.* **1981**, *19*, 1687–1704.
- (25) Hsu, W. Y.; Gierke, T. D. *Macromolecules* **1982**, *15*, 101–105.
- (26) Marx, C. L.; Caulfield, D. F.; Cooper, S. J. *Macromolecules* **2000**, *33*, 6541–6550.
- (27) Porat, R.; Fryer, J. R.; Huxham, M.; Rubinstein, I. *J. Phys. Chem.* **1995**, *99*, 4667–4671.
- (28) Chomakova-Haefke, M.; Nyffenegger, R.; Schmidt, E. *Appl. Phys. A* **1994**, *59*, 151–153.
- (29) Bath, B. D.; Lee, R. D.; White, H. S. *Anal. Chem.* **1998**, *70*, 1047–1058.
- (30) Collette, F. M.; Lorentz, C.; Gebel, G.; Thominette, F. *J. Membr. Sci.* **2009**, *330*, 21–29.
- (31) Marrony, M.; Barrera, R.; Quenet, S.; Ginocchio, S.; Montelatici, L.; Aslanides, A. *J. Power Sources* **2008**, *182*, 469–475.
- (32) Kundu, S.; Simon, L. C.; Fowler, M. W. *Polym. Degrad. Stab.* **2008**, *93*, 214–224.
- (33) Qiao, J.; Saito, M.; Hayamizu, K.; Okada, T. *J. Electrochem. Soc.* **2006**, *153*, A967–974.
- (34) Knight, S. D.; Colbow, K. M.; St-Pierre, J.; Wilkinsom, D. P. *J. Power Sources* **2004**, *127*, 127–134.
- (35) Alentiv, A.; Kostina, J.; Bondarenko, G. *Desalination* **2006**, *200*, 32–33.
- (36) O’Hayre, R.; Lee, M.; Prinz, F. B. *J. Appl. Phys.* **2004**, *95*, 8382–8392.
- (37) Nguyen, T. V.; Nguyen, M. V.; Lin, G.; Rao, N.; Xie, X.; Zhu, D.-M. *Electrochim. Solid-State Lett.* **2006**, *9*, A88–A91.
- (38) Xie, X.; Kwon, O.; Zhu, D.-M.; Nguyen, T. V.; Lin, G. *J. Phys. Chem. B* **2007**, *111*, 6134–6142.
- (39) Kang, Y.; Kwan, O.; Xie, X.; Zhu, D.-M. *J. Phys. Chem. B* **2009**, *113*, 15040–15046.
- (40) Bussian, D. A.; O’Dea, J. R.; Metiu, H.; Buratto, S. K. *Nano Lett.* **2007**, *7*, 227–232.
- (41) McLean, R. S.; Doyle, M.; Sauer, B. B. *Macromolecules* **2000**, *33*, 6541–6550.
- (42) Lehmani, A.; Durand-vidal, S.; Turq, P. *J. Appl. Polym. Sci.* **1998**, *68*, 503–508.
- (43) James, P. J.; Elliott, J. A.; McMaster, T. J.; Newton, J. M.; Elliott, A. M. S.; Hanna, S.; Miles, M. J. *J. Mater. Sci.* **2000**, *35*, 5111–5119.
- (44) Haight, F. A. *Handbook of the Poisson Distribution*; Wiley: 1967; p 168.
- (45) PicoScan and 5500 Atomic Force Microscopes, Agilent Technology, 4666 S. Ash Ave, Tempe, AZ 85282.
- (46) DuPont Nafion Products, 22828 NC 87 Hwy W., Fayetteville, NC 28306.
- (47) Clean Fuel Cell Energy, LLC, P.O. Box 6713, Clearwater, FL 33758 (<http://www.cleanfuelcellenergy.com/membrane.html>).
- (48) Yang, C.; Srinivasan, S.; Bocarsly, A. B.; Tulyani, S.; Benziger, J. B. *J. Membr. Sci.* **2004**, *237*, 145–161.
- (49) Orfino, F. P.; Holdcroft, S. *J. New Mater. Electrochim. Syst.* **2000**, *3*, 287.

JP911182Q